Reduction of Metal Artifacts in Computed Tomographies for the Planning and Simulation of Radiation Therapy

T. Rohlfing[a∗], D. Zerfowski[b†], J. Beier[a∗], P. Wust[a‡], N. Hosten[a], R. Felix[a]

[a]Department of Radiology, Charité, Campus Virchow-Klinikum,
Augustenburger Platz 1, D-13353 Berlin, Germany

[b]Universität Karlsruhe, Institut für Algorithmen und Kognitive Systeme,
Am Fasanengarten 5, D-76131 Karlsruhe, Germany

ABSTRACT

Subject was to evaluate techniques for the reduction of metal artifacts in X-ray computed tomographies (CT). Compared to simulated CT projection data, real measurements allowed less improvements in image quality. Neither could metal artifacts be eliminated completely, nor was there a significant gain regarding the presentation of anatomical structures in the immediate neighbourhood of metal objects. Reduction of global image noise, however, was clearly recognizable. For further processing of the tomographies including several applications in the field of radiation therapy, this promises improved accuracy and numerical stability.

1. INTRODUCTION

In radiation therapy, computed tomographies are used for patient positioning as well as for treatment planning by simulation of dose distribution. For these applications, artifacts caused by all kinds of metallic implants (teeth fillings, prostheses, fiducial markers, etc.) impose severe limitations upon the reliability of the results.

A variety of different techniques for the reduction of metal artifacts in computed tomographies exist. Methods for post-processing of artifact-containing images like a template-based approach by Morin and Raeside [1] were not very successful.

Most effective algorithms work on raw projection data, i.e. the set of ray attenuations measured by the CT scanner. Kalender et al. [2] interpolated missing projections and afterwards used standard filtered backprojection for artifact reduced image reconstruction. Identification of incorrectly measured rays was done by manual identifaction of metal objects in the uncorrected reconstructions.

Other approaches had the operator define a threshold value for measurements to be

∗Supported by Deutsche Forschungsgemeinschaft GRK 331/1-97
†Supported by Deutsche Forschungsgemeinschaft SFB 414
‡Supported by Deutsche Forschungsgemeinschaft SFB 273

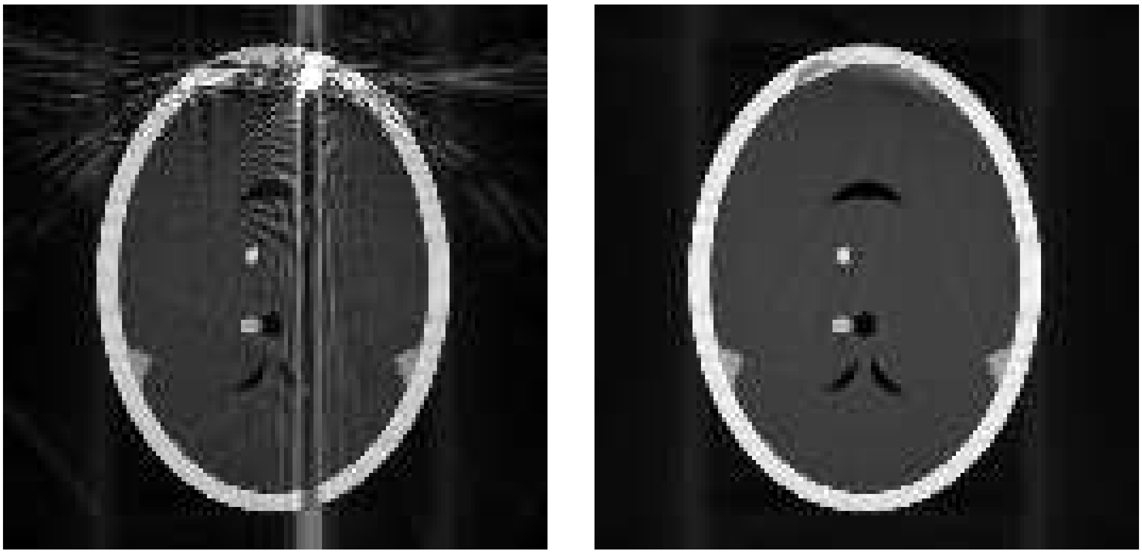

Figure 1. Reconstructions from simulated projection data. A head phantom with a simulated metal implant (located in the top right part of the skull) was scanned using the TomAS tomography simulator [6]. Reconstruction to a 512×512 pixel matrix was performed by Fourier reconstruction with native data (left) and linearly interpolated missing projections (right).

corrected. Requiring even less user interaction, a modification to these methods recently presented by Zerfowski [3] determined the disturbed projections by analysis of the raw data histogram.

Compared with continuous integral transform methods, iterative discrete reconstruction algorithms allow explicit modeling of imperfect real-world data. In the simplest case, missing projections are simply ignored. A more sophisticated approach was used for example by Wang et al. [4,5]. Their so-called iterative deblurring scheme, besides other modifications, calculated spatially local relaxation coefficients depending on the presence of metal in the reconstruction area.

2. MATERIALS AND METHODS

Simulated projection data for the reconstructions shown in Fig. 1 was collected using the TomAS tomography simulator package by Zerfowski et al. [6]. A parallel-beam scanner calculated pseudo-projections of 512 detectors for 512 views covering 180°.

Acquisition of real patient data was performed using a Siemens Somatom Plus S CT scanner (Siemens Medical Engineering, Forchheim, Germany). For each slice, 1242 views covered a full rotation with no intermediate table movement. Within each view, 1536 measurements were collected with a fan-beam geometry, 42.6° being the fan angle. Projection data for the images in Fig. 2 was measured with the scanner gantry tilted by 25°.

Image reconstruction operators were implemented into the commercially available visu-

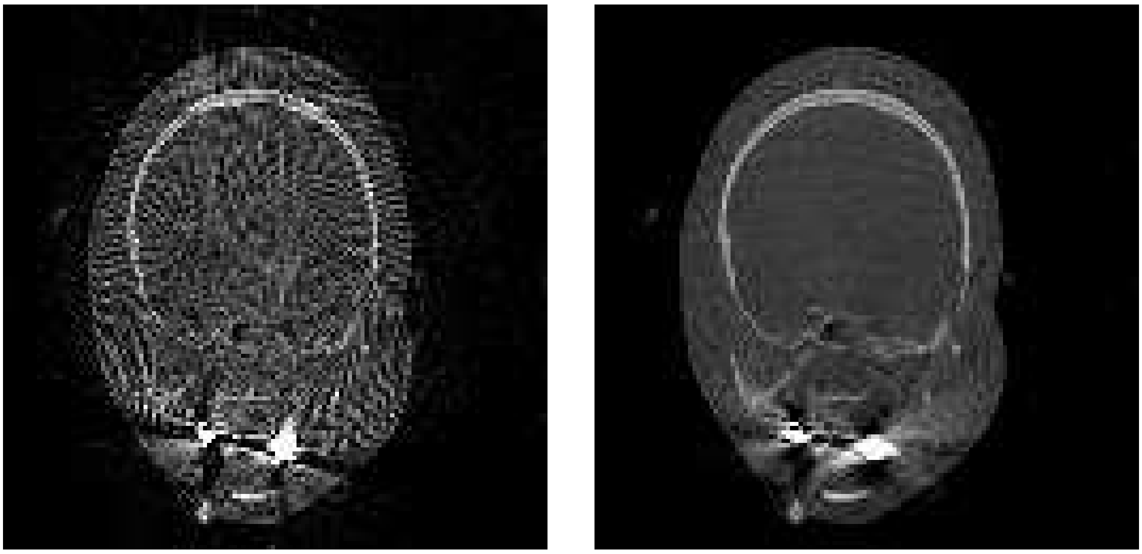

Figure 2. Computed tomographies from real projection data. Reconstruction was done using filtered backprojection with an edge-enhancing generalized Hamming filter (parameter $\alpha = 2$). Shown on the left is the image calculated from native (i.e. uncorrected) raw data. For the image on the right, missing projections were linearly interpolated before FBP. Both images consist of 512×512 pixels. The field of view (FOV) was 300×300mm, equivalent to a spatial resolution of 0.59mm.

alization and imaging development environment AVS/Express (Advanced Visual Systems, Waltham, MA, USA). Computation times given refer to an SGI O2 workstation (Silicon Graphics, Mountain View, CA, USA).

For reconstruction by filtered backprojection (FBP), the raw projection data was bilinearly interpolated from the scanner's fan-beam geometry to the same number of views covering 360° with 1536 equally spaced parallel rays per view.

Artifact reduction with FBP reconstruction was achieved by linear interpolation of missing projection data as proposed by Kalender et al. [2]. Metal-affected measurements were identified using a manually chosen constant threshold.

As a sample iterative technique, additive algebraic reconstruction (ART) was implemented for both the scanner's native fan-beam geometry and the virtual parallel geometry used by FBP. In both cases, metal artifacts were supressed by ignoring projections exceeding the same threshold level chosen for interpolation before application of FBP.

3. RESULTS

An example for the effects of interpolation of missing measurements upon reconstruction quality is shown in Fig. 1 for simulated projection data. Streak artifacts disappeared almost completely, even in the immediate neighbourhood of the metal object. However, the metal object itself also disappeared.

For a real patient with metallic teeth fillings, sample head CTs are shown in Fig. 2. It

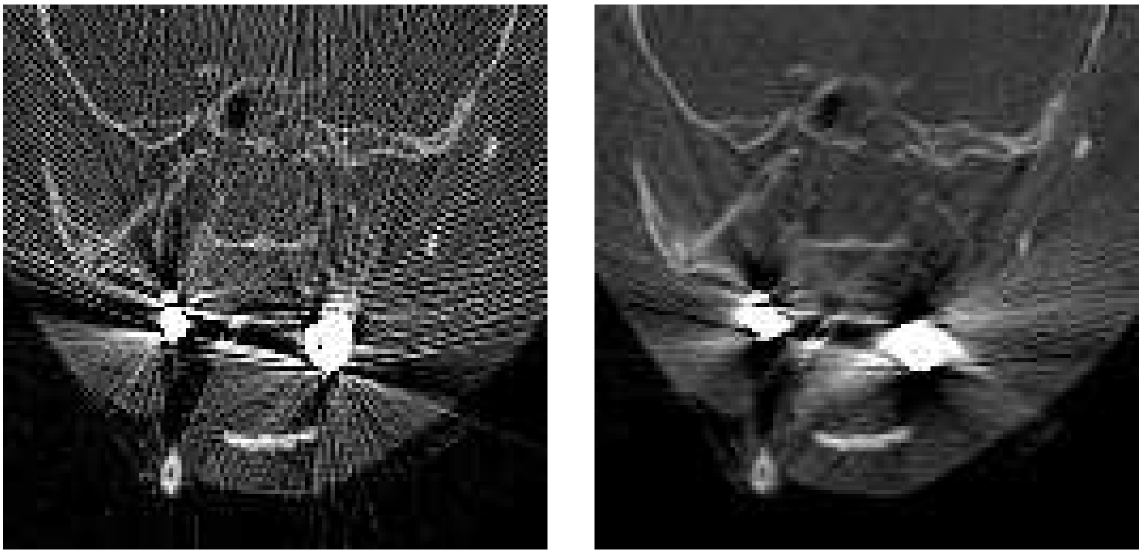

Figure 3. Details from the computed tomographies in Fig. 2. Both reconstructions were performed with a restricted FOV (165×165mm), resulting in a resolution of 0.32mm (512×512 pixels). FBP parameters were identical to those used for Fig. 2. Again, for the right image missing projection data was linearly interpolated.

should be noticed that this patient had been the victim of an accident. This accounts for some unusual structures that may at first sight look like artifacts but are real objects (i.e. injury at the bottom left of the chin).

Artifact reduction by interpolation of missing projection data significantly reduces the overall image noise with no obvious loss in contrast or spatial resolution. Especially in regions not directly adjacent to the metal objects there is an increase in image quality. Anatomic details previously concealed can be identified after artifact suppression. Skin surface, for example, is presented as a more closed border against the surrounding air.

For statistical analysis a region of interest (ROI) was defined, covering 100×100 pixels top right of the head in the CTs from Fig. 2. This region was chosen to contain only surrounding air, thus Hounsfield values in the reconstruction should be close to -1000 HU.

Before artifact reduction, values ranged from -1197 HU to -869 HU with a mean of -972 HU and a standard deviation of 38.8 HU. Reconstruction of the corrected projection data produced values ranging from -1091 HU to -970 HU. While the mean value changed only slightly to -971 HU after artifact reduction, standard deviation was reduced to 13.5 HU.

In addition, Fig. 4 presents the detail reconstructions of the metal objects from Fig. 3 with an extended grey level window adapted to bone structures. It can be seen that the total intensities of the metal objects themselves have been decreased.

No sample images are given for ART, because it was not possible to produce visually sufficient reconstructions within a sensible computing time ($>$ 5 hours). Reconstruction by FBP required 5 minutes for each of the images shown in this paper (implementation was not optimized for speed). Difference between native and artifact reduced application

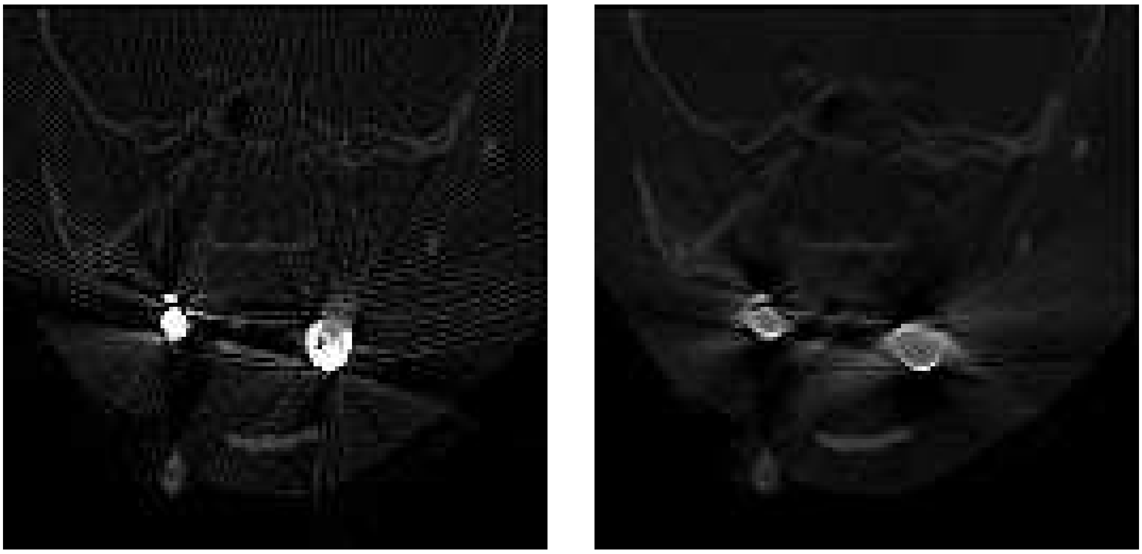

Figure 4. Details of the computed tomographies from real projection data in Fig. 3 displayed with an extended grey level window (range -1000 HU – +1000 HU). Left: reconstruction from native projection data, right: after linear interpolation of missing projections.

of FBP was less than 5 seconds for the additional thresholded interpolation of missing projections. Pipelining with FBP itself is possible, further decreasing additional computation time to almost zero.

4. CONCLUSIONS

Reduction of streak artifacts from metal objects in CT is generally possible. Even simple modifications such as interpolation of missing projections leads to visible improvements with almost no additional computational effort.

Results from tests with simulated raw data obviously cannot be transferred to clinical application. An increase in image quality comparable to that seen in Fig. 1 cannot be achieved for real projection data. Explanations might be the impact of physical sources of error (noise, photon statistics, beam hardening) or insufficient modeling of metal objects in the simulation.

Nevertheless, statistical analysis of a homogeneous ROI showed that image noise is significantly reduced and intensity extrema are cut off for reconstructions from real projection data as well. Both effects support the accuracy and numerical stability of further calculations.

Presentation of anatomical details on the other hand is very little disturbed by artifact reduction, especially in some distance from the metal objects. The effect is therefore superior to elimination of noise and streak artifacts by a smoothing filter. Further benefits include clearer presentation of at least some object boundaries (skin surface). This could be helpful for other applications as for example image segmentation.

Visual impression from Fig. 4 indicates that all this can be achieved even by simple interpolation of missing projection data. Compared to filtered backprojection of this corrected raw data, we found that iterative algebraic reconstruction techniques suffer from limitations that make them impractical for use in clinical routine at least today.

First of all, one may well be able to have 20 or more iterations of an iterative reconstruction technique be performed when generating a 128×128 pixel image from some thousand measurements. Given more than 1.8 million measured rays and expecting a 1024×1024 image, computing time sets a bound of hardly more than 5 iterations.

In addition, algebraic reconstruction is unable to focus on some small FOV as filtered backprojection can. It is therefore inevitable to consider the CT scanner's reconstruction area (generally large) as a whole. For the Siemens Somatom scanner used by the authors, this would imply reconstruction to a 1600×1600 matrix to achieve a resolution similar to that of the detail images in Fig. 2.

5. ACKNOWLEDGEMENTS

The authors would like to thank E. Klotz of Siemens Medical Engineering Group CT (Forchheim, Germany) for kind assistance with the Somatom data file formats and scanner geometry.

REFERENCES

1. R. L. Morin and D. E. Raeside, A Pattern Recognition Method for the Removal of Streaking Artifact in Computed Tomography, Radiology **141**, 229–233 (1981).
2. W. A. Kalender, R. Hebele, and J. Ebersberger, Reduction of CT artifacts caused by metallic implants, Radiology **164**(2), 576–577 (1987).
3. D. Zerfowski, Kompensation von Metallartefakten in der Computertomographie. In: *Proceedings zum Workshop: Bildverarbeitung für die Medizin 1998*, Informatik Aktuell, Springer, 1998.
4. G. Wang, D. L. Snyder, and M. W. Vannier, Local Computed Tomography via Iterative Deblurring, Scanning **18**, 582–588 (1996).
5. G. Wang, D. L. Snyder, J. A. O'Sullivan, and M. W. Vannier, Iterative Deblurring for CT Metal Artifact Reduction, IEEE Transactions on Medical Imaging **15**, 657–664 (1996).
6. D. Zerfowski, T. Rohlfing, U. Mende, and T. Beth, TomAS – Tomographic Algorithms and Ultrasound Simulation. In: *Computer Assisted Radiology and Surgery 97*, Ed. H.U. Lemke, M.W. Vannier, and K. Inamura, Berlin, June 1997.